Drying Technology: An International Journal
Publication details, including instructions for authors and subscription information:
http://www.tandfonline.com/loi/ldrt20

Investigation on Convective Drying of Mixtures of Sewage Sludge and Sawdust in a Fixed Bed

Jie Li[a], Laurent Fraikin[a], Thierry Salmon[a], Lyes Bennamoun[ab], Dominique Toye[a], Raphael Schreinemachers[c] & Angélique Léonard[a]

[a] Laboratory of Chemical Engineering, Department of Applied Chemistry, University of Liège, Liège, Belgium

[b] Department of Mechanical Engineering, Faculty of Engineering, University of New Brunswick, Fredericton, NB, Canada

[c] Industrie du Bois Vielsalm & Cie SA, Zoning Industriel de Burtonville, Vielsalm, Belgium

Accepted author version posted online: 05 Nov 2014.

To cite this article: Jie Li, Laurent Fraikin, Thierry Salmon, Lyes Bennamoun, Dominique Toye, Raphael Schreinemachers & Angélique Léonard (2014): Investigation on Convective Drying of Mixtures of Sewage Sludge and Sawdust in a Fixed Bed, Drying Technology: An International Journal, DOI: 10.1080/07373937.2014.982254

To link to this article: http://dx.doi.org/10.1080/07373937.2014.982254

Investigation on Convective Drying of Mixtures of Sewage Sludge and Sawdust in a Fixed Bed

Jie Li[1,], Laurent Fraikin[1], Thierry Salmon[1], Lyes Bennamoun[1,2], Dominique Toye[1], Raphael Schreinemachers[3], Angélique Léonard[1]

[1]Laboratory of Chemical Engineering, Department of Applied Chemistry, University of Liège, Liège, Belgium, [2]Department of Mechanical Engineering, Faculty of Engineering, University of New Brunswick, Fredericton, NB, Canada, [3]Industrie du Bois Vielsalm & Cie SA, Zoning Industriel de Burtonville, Vielsalm, Belgium

Corresponding author. E-mail address: jie.li@ulg.ac.be

Abstract

This work is a part of a project aiming at developing a renewable fuel for gasification purposes, through convective drying of sludge/wood mixtures. The first step consists of characterizing the behavior of sawdust/sludge mixtures during the application of convective drying. The influence of the mixing step (no mixing against 30 s at 40 rpm), as well as the sawdust/sludge ratio (1/9, 2/8, 3/7 and 4/6 on a dry basis) and the effect of the drying temperature (50 °C, 80 °C and 110 °C) have been investigated. In this study, X-ray tomography, a non-invasive imaging technique, is used to assess changes in the volume, void and exchange surface at the beginning and the end of the drying process. Results first confirm the importance of the mixing step on the drying behavior: the drying rate of the mixed sludge is lower than that of the original sludge. Nevertheless the addition of sawdust is shown to have a positive impact on the drying process from a mass ratio of 2/8, with drying rates higher than that of the original sludge. With increasing amount of sawdust, the initial and final bed volumes, initial and final total exchange

surfaces, and initial void fraction increase linearly, but the bed volume shrinkage and final void fraction decrease linearly.

KEYWORDS: Sewage sludge; Sawdust; Convective drying; Mixing; Shrinkage; X-ray tomography

INTRODUCTION

Because of the increased water demand of the world's population, together with stringent requirements for discharge into the natural environment, the quantity of sludge generated from wastewater treatment plants (WWTPs) is continuously increasing [1, 2]. Hence, the valorization of sludge has become a critical issue. In the past years, many technologies have been used for sludge valorization, such as land application, composting and incineration. However, the high moisture content of sludge is still considered as a critical parameter that governs the feasibility of various final disposal routes [3]. It is now well established that thermal drying operation, after mechanical dewatering, is an essential step prior to current sludge valorization options. Léonard et al. [4–7] investigated the convective drying of wastewater sludge dried in a rig. Moreover, they also studied the influence of air temperature, superficial velocity, and humidity on the drying kinetics and on shrinkage and cracks formation using X-ray microtomoraphy. This technique has also been used by other teams for similar types of studies. Tao et al. [8–10] investigated the volume shrinkage and crack development by X-ray microtomography in thermal drying of wastewater sludge. It was found that the volume shrinkage decreased the drying area but the crack development increased the drying area. Arlabosse et al. [11] developed an

experimental methodology to improve the design of paddle dryers. A good agreement was obtained between the experimental and modeling results. Simulation works regarding sludge drying were also developed by researchers [12–16]. The water diffusion coefficient during wastewater sludge drying was determined by comparing experimental data with the analytical solution of the diffusion equation [12, 13]. Furthermore, the shrinkage effect was introduced to the modeling and simulation of heat and mass transfer during convective drying of wastewater sludge [14, 15]. An advanced finite-element simulation with three-dimensional volumetric grids was studied and the heat and mass transfer processes in the drying of wastewater sludge cake were simulated [16]. Nevertheless there are still some attempts to find new valorization routes for sludge.

In this work, it is proposed to generate an original renewable fuel that could enter a gasification process, by drying a mixture of sludge with sawdust. Adding sawdust is expected to be a way of reinforcing the texture of soft and pasty sludge which is difficult to dry. Reinforcing the texture of sludge can increase the drying rate and decrease the drying time, and then the heat energy supply may be reduced significantly. Based on the previous study dealing with back mixing [17], where it was found that expansion of the sludge bed enhanced heat and mass transfer, we expect positive results using the approach of mixing sludge with sawdust. Furthermore, sawdust brings organic matter which is useful for gasification. This material is produced in large amount by the forest industry and also needs safe disposal solutions [18]. Usually, sawdust is applied in the manufacture of compressed biofuels or for making compressed wood boards [19], but new applications should be explored. A mixing machine can be added to the typical

industrial sludge drying setup which consists of a belt dryer and sludge extruder. Sawdust/sludge mixtures are extruded and then dried in the belt dryer. The investment cost will slightly increase because of the addition of the mixing machine. However, as mentioned above the operation cost may be reduced significantly in the ideal condition because the reduction of the drying time. Altogether, the overall cost is speculated to be reduced. Finally, the removal of water during drying is essential prior to gasification, in order to reach a calorific value adapted to such thermochemical conversion process [20].

The present work aims to determine the effect of sawdust addition operation on the convective drying kinetics of wastewater sludge. X-ray tomography, a non-destructive imaging technique, is used to follow the 3D characteristics, in particular volume [21–24], exchange surface [17, 21–23, 25], and void fraction [17, 26, 27].

MATERIALS AND METHODS

Materials

Sludge was collected after mechanical dewatering step in a WWTP located near the University of Liège (Grosses Battes, Belgium). The initial moisture content was determined according to standard methods [28] with a value around 85.5% (wet basis). Before drying, the sludge was stored at a temperature of 4 °C, to keep the same properties during storage [29]. Table 1 provides physical and chemical characteristics of the sludge used.

Pine sawdust was collected from a wood pellet factory ('Industrie du bois', Vielsalm, Belgium) and the initial moisture content (wet basis) was around 30%. Table 2 gives the size distribution of the sawdust used.

In this study, the drying behavior of several samples was tested: the original sludge, the mixed sludge (the original sludge after mixing without sawdust), and mixtures (the original sludge after mixing with sawdust). A kitchen machine (KM1000, PROline) with a beater was used to prepare the mixed sludge and sawdust/sludge mixtures. The mass ratios (expressed on a dry matter basis for both sludge and sawdust) of sawdust/sludge were 1/9, 2/8, 3/7, and 4/6. The addition of sawdust changed the structure and property of the sample bed submitted to drying [30]. In previous studies [17, 31], it was found that back mixing and liming changed the rheological property of sludge, in relation with the structure of the bed. In particular, the cohesion of sludge decreased with longer mixing time and higher mixing velocity. Consequently, the rigidity of sludge extrudates decreased, producing fixed beds of the product with smaller exchange areas, and leading to the decrease of the drying rate. In our study, a low mixing rate (40 rpm) and a short mixing time (30 s) were chosen for a compromise. The same protocol was used to mix the original sludge without any sawdust addition for preparing the mixed sludge. Before drying, these samples were extruded through a disk with circular dies of 12 mm, forming a bed of extrudates on the dryer perforated grid. The initial mass of the extrudates bed was fixed at 500 g in all experiments. By doing it this way, it is assessed that the corresponding industrial belt dryer would operate at constant feeding rate, on a global mass basis. The results will be interpreted consequently.

Pilot-Scale Dryer

Drying experiments were carried out in a discontinuous pilot-scale dryer reproducing most of operating conditions prevailing in a full-scale continuous belt dryer, as shown in Fig. 1. A fan (a) draws in ambient air and then the air is heated up to the required temperature by a set of electrical resistances (b). If needed, the air is humidified after heating by adding vapor from a vapor generator. The hot air flows through the sludge extrudates (c), which lies on a perforated grid (d) linked to a scale (e). The inner diameter of the sample holder is 160 mm. The sludge sample forms a packed bed with an initial height ranging from ~40 to ~60 mm with increasing amount of sawdust. Three operating parameters can be controlled: air temperature, superficial velocity, and humidity. In this study, three temperatures were used: 50 °C, 80 °C and 110 °C, with air velocity fixed at 2 m/s and no additional air humidification. During the entire study, the ambient air humidity was close to 0.004 $kg_{water}/kg_{dry\ air}$. The sample remained in the same vessel and was continuously weighed during the entire drying test. The mass was recorded every 10 s.

X-Ray Tomography

X-ray tomography was used to determine the influence of sawdust addition on the structure of the extrudates bed. This non-invasive technique, originally developed for medical applications, allows for obtaining 2D cross-sections and 3D images of the bed. The volume, void fraction and total exchange surface available for heat and mass transfer were determined by image analysis of the tomographic images.

The X-ray tomographic device used in this study is a high-energy X-ray tomograph, first presented by Toye et al. [32]. The generator is a Baltograph CS450A (Balteau NDT, Belgium), which can operate between 30 and 420 kV. The X-ray source is an oil-cooled, bipolar TSD420/0 tube (Comet and Balteau NDT). The intensity can be varied between 2 and 8 mA depending on the voltage used. A lead collimator produces a 1 mm thick fan beam. The detector is an X-Scan 0.4f2-512-HE manufactured by Detection Technology (Finland). This detector consists of a linear array of 1280 photodiodes each coupled with a $CdWO_4$ scintillator. The mechanical rig designed by Pro Actis, Belgium, consists of two parts, a source–detector arm and a rotating table on which the object to be scanned is fixed. This arm is embedded in a carriage that slides on two vertical high precision machined rails. The rig allows vertical movement up to 3780 mm, keeping vertical and horizontal errors within 1 mm. The maximum diameter of the sample that can be tested is 0.45 m.

The extrudates bed to be scanned is placed on the rotating table whose rotation is obtained by a synchronous motor equipped with a frequency validator which is supervised by the data acquisition system. Once the extrudates bed is put on the rotating table, 1D X-ray acquisitions of the bed are recorded around 360°. Tomographic reconstruction of the cross-sections was obtained by a classical linear back-projection algorithm adapted to the fan beam geometry and implemented in the Fourier domain. When the 2D reconstructed cross-sections are stacked, they provide a 3D X-ray attenuation map of the bed.

In our experiments, the energy of the source was fixed at 420 kV and 3.5 mA, the pixel size of the image was 0.36 mm, and the height interval was 2.2 mm.

Image Analysis

Gray-level images provided by X-ray tomography are formed by two phases: the void space at low gray levels (dark pixels) and sludge extrudates at high gray levels (bright pixels). A circular mask corresponding to the inner diameter of the drying chamber was first constructed to isolate the sludge bed from the background. Then binarization, i.e. assigning the value 1 to pixels belonging to the sludge and the value 0 to pixels belonging to the void, was performed following Otsu's method [33]. The calculation methods of the bed volume, void fraction and total exchange surface are as follows [17, 25, 30]:

The bed volume was the total volume of solid and void in the volume-of-interest (VOI). The calculation method was the total number of voxels of solid and void space in the VOI timed the volume of a voxel.

The void fraction was determined by dividing the number of pixels corresponding to the void space by the total number of pixels of VOI (void +solid).

The total exchange surface was calculated by the total perimeter of the air/solid interface in 2D cross-sections, i.e. the pixel edges shared by void and solid pixels, timed the distance between two slices.

All these operations were implemented in Matlab (Matworks), using the image analysis toolbox version 6.0.

RESULTS AND DISCUSSION

Drying Behavior

The influence of the mixing step (no mixing against 30 s at 40 rpm), as well as the sawdust/sludge ratio (1/9, 2/8, 3/7 and 4/6 on a dry basis) and the effect of the drying temperature (50 °C, 80 °C and 110 °C) have been investigated. Fig. 2 shows the drying rate vs. moisture content of sludge. As can be seen, regular patterns of the drying rate curves are almost the same at different drying temperatures. However, it is clear that higher drying rates are obtained with higher temperature. Moreover, this figure shows that for the three temperatures the drying rate is lower for the sludge after mixing. Nevertheless, with the addition of sawdust the drying rate recovers and even increases.

In order to compare the drying kinetics of different samples, drying characteristics including the total amount of sludge, normalized amount of sludge, sludge flow rate, total amount of evaporated water, normalized amount of water, drying time, normalized drying time, average drying rate, and normalized drying rate are shown in Table 3. The average drying rate during the drying process was calculated by dividing the total amount of evaporated water by the drying time. The normalized values were calculated using the value of the original sludge as a reference. The total amount of sludge and the total amount of evaporated water of the original sludge and mixed sludge are the same.

However, the drying time significantly increases after the mixing step and then the average drying rate of the mixed sludge is significant lower than that of the original sludge. This result confirms the negative effect of the mixing step on the sludge drying behavior [34]. As mentioned above, the initial mass of the bed of extrudates was fixed at 500 g in all experiments, so the total amount of sludge decreases with increasing amount of sawdust (from 500 to 439 g). Furthermore, because the moisture content of sawdust is far lower than that of sludge, the total amount of evaporated water presented in the mixture also decreases (from 425 to 390 g at 50 °C) with increasing amount of sawdust. However, the drying time decreases more uncommonly with increasing amount of sawdust resulting in higher average drying rate (up to a factor 1.622 at 50°C). This means that the addition of sawdust changes the structure of the sample bed and has a positive impact on the drying process from a mass ratio of 2/8, with observed drying rates higher than those of the original sludge. Indeed, because for the mixtures the amount of sludge decreases with increasing amount of sawdust, if the same amount of sludge is treated, the sludge flow rate should be increased. For example, for the mass ratio of 2/8, the sludge flow rate should be increased by a factor of 1.053, but at the same time the average drying rate increases by a factor 1.121 (at 50°C) which is higher, so the drying is clearly enhanced. Altogether, the positive effect of the addition of sawdust is clearly observed: for different drying temperatures, the drying rate generally increases with increasing amount of sawdust, while the initial water content as well as the total amount of water to be removed both decrease. Indeed the same initial mass of the bed of extrudates is introduced for each experiment.

Typically, during convective drying of wastewater sludge, three periods are observed, as presented in the experimental works completed by Léonard et al. [4, 6], Vaxelaire and Puiggali [35], Reyes et al. [12], and Bennamoun et al. [14, 15].

1. First drying period, also called the preheating period: It is a short lapse of time reflecting the adaptation of the product to the new, applied process conditions characterized by a high increase in the evaporation flux, as shown in Fig. 2.

2. Second drying period, called the constant drying rate period: It is obvious that this period is very short in the drying experiments, as shown in Fig. 2. During this constant rate period the evaporation takes place at the surface of the wet solid, and the solid assumes a constant equilibrium temperature, just as a free liquid surface is maintained at the wet-bulb temperature of the air [36]. In most published papers, the surface change related to shrinkage is not taken in consideration in this period.

3. Third drying period, known as the falling drying rate period: It is a long period, as illustrated in Fig. 2. The water removed in this period is interstitial water at first, followed by surface water, and then bound water [37]. Sherwood [36] has divided the falling rate period into two zones: zone of decreasing wetted surface and zone of controlling internal liquid diffusion.

Altogether, the drying kinetics of sludges and sawdust/sludge mixtures are similar, which have a short preheating period, a short constant drying rate period, and a long falling drying rate period. More research of drying behavior is shown in one previous work [38].

Bed Volume and Shrinkage

As mentioned above, X-ray tomography is used to assess changes in the volume, void, and exchange surface. Fig. 3 shows an example of the image of the 2D cross-section and 3D reconstruction image of the bed of the original sludge before drying.

The apparent volumes occupied by the sample bed before and after drying vs. ratio of sawdust/sludge at different drying temperatures are shown in Fig. 4. The regular patterns of bed volumes are almost the same for the three drying temperatures. When performing a mixing step, the initial bed volume slightly decreases. This is because the mixing step presses the sludge and then the density of sludge increases. Moreover, the initial and final volumes both increase linearly with increasing amount of sawdust. This is because sawdust reinforces the texture of sludge. The linear fitting method was used for the results of the mixed sludge and sawdust/sludge mixtures. The fitting results including the linear correlation coefficients and linear fitting equations are shown in Table 4. The linear correlation coefficients are good and close to 1.

It is worth mentioning that the results of the initial bed volume (void fraction and total exchange surface) for the three drying temperatures should be the same in theory, but it was difficult to generate reproducible beds. For this reason, it was not possible to get exactly the same results. However, the difference of the results of the initial bed volume is small (see in Fig. 4) and the relative deviation of the three bed volumes for the three

drying temperatures is 4.79%. This means the results of the X-ray tomography are repeatable and reliable.

By comparing the bed volume before and after drying, it is obvious that a high shrinkage occurs for each sample. Shrinkage can be quantified as the ratio between the initial and final volumes, noted ε and defined as:

$$\varepsilon = \frac{V_1 - V_2}{V_1} \quad (1)$$

In Eq. (1), V_1 and V_2 are the initial and final bed volumes, respectively.

Fig. 5 shows the bed volume shrinkage vs. ratio of sawdust/sludge at different drying temperatures. First of all, with the mixing step the bed volume shrinkage slightly decreases. Second, the bed volume shrinkage decreases linearly with increasing amount of sawdust. This means that sawdust braces the structure of the sample bed during drying. The linear fitting results of the bed volume shrinkage of the mixed sludge and sawdust/sludge mixtures are shown in Table 5 and the linear correlation coefficients are good and close to 1.

By comparing the results at different drying temperatures, the bed volume shrinkage obtained for the same mass ratio of sawdust/sludge is smaller when the drying temperature is higher. This can be easily explained by a 'crust formation' phenomenon [39, 40].

More results and deeper discussion about shrinkage phenomenon occurring during this sawdust/sludge drying process have already shown in previous works [30, 38].

Void and Total Exchange Surface

The variations of the void fraction and total exchange surface before and after drying were also investigated. Fig. 6 shows the results of the void fraction before and after drying vs. ratio of sawdust/sludge at different drying temperatures. For the three drying temperatures, the regular patterns are almost the same. The difference of the initial and final void fractions between the original sludge and mixed sludge is not significant. However, the initial void fraction significantly increases and the final void fraction slightly decreases with increasing amount of sawdust. The linear fitting results of the void fraction of the mixed sludge and sawdust/sludge mixtures are shown in Table 6. Most of the linear correlation coefficients are good and close to 1.

It is worth mentioning that the void fraction was determined by dividing the void volume by the bed volume (void volume + solid volume) and it is a relative value. Since the final bed volume and final void fraction were both obtained, the final void volume can be calculated and the results are shown in Table 7. It is shown that the final void volume increases with increasing amount of sawdust for the three drying temperatures.

Fig. 7 shows the results of the total exchange surface before and after drying vs. ratio of sawdust/sludge at different drying temperatures. When performing the mixing step, the initial total exchange surface significantly decreases. Moreover, the initial and final total

exchange surfaces for the three drying temperatures both increase linearly with increasing amount of sawdust. The linear fitting results of the total exchange surface of the mixed sludge and sawdust/sludge mixtures are shown in Table 8. The linear correlation coefficients are good and close to 1.

CONCLUSIONS

This work investigated the influence of sawdust addition on convective drying of sewage sludge. The mixing step has a negative impact on the drying process. Nevertheless, sawdust addition is shown to have a positive impact on the drying process from a mass ratio of 2/8. Moreover, the drying rate generally increases with increasing amount of sawdust.

After the mixing step, the initial bed volume and shrinkage both slightly decrease, but the total exchange surface significantly decreases. With increasing amount of sawdust, the initial and final bed volumes, initial and final total exchange surfaces, and initial void fraction increase linearly, but the bed volume shrinkage and final void fraction decrease linearly. Sawdust reinforces the texture of sludge.

Further work will be done in order to characterize pore textures of the single extrudate of different samples. The behavior of these samples during pyrolysis using thermo gravimetric analysis will also be investigated.

ACKNOWLEDGMENTS

J. Li is grateful to University of Liège for a postdoctoral grant. L. Fraikin and L. Bennamoun are thankful to the FRS-FNRS for their postdoctoral fellow positions (FRFC projects 2.4596.12 and 2.4596.10).

REFERENCES

1. Vesilind, P.A.; Spinosa, L. Production and regulations. In *Sludge into biosolids, Processing, Disposal and Utilization*, Spinosa, L.; Vesilind, P.A. Eds., IWA Publishing, London, 2001, 3–18.
2. Spinosa, L. Evolution of sewage sludge regulations in Europe. *Water Science and Technology* **2001**, 44(10), 1–8.
3. Lee, D.J.; Liu, J.C. Route to synthesize the sludge management processes. *Water Science and Technology* **2004**, 49(10), 259–266.
4. Léonard, A.; Blacher, S.; Marchot, P.; Crine, M. Use of X-ray microtomography to follow the convective heat drying of wastewater sludges. *Drying Technology* **2002**, 20(4–5), 1053–1069.
5. Léonard, A.; Blacher, S.; Pirard, R.; Marchot, P.; Pirard, J.P.; Crine, M. Multiscale texture characterization of wastewater sludges dried in a convective rig. *Drying Technology* **2003**, 21(8), 1507–1526.
6. Léonard, A.; Blacher, S.; Marchot, P.; Pirard, J.P.; Crine, M. Measurement of shrinkage and cracks associated to convective drying of soft materials by X-ray microtomography. *Drying Technology* **2004**, 22(7), 1695–1708.
7. Léonard, A.; Blacher, S.; Marchot, P.; Pirard, J.P.; Crine, M. Convective drying of wastewater sludges: Influence of air temperature, superficial velocity, and humidity

on the kinetics. *Drying Technology* **2005**, 23(8), 1667–1679.

8. Tao, T.; Peng, X.F.; Lee, D.J. Thermal drying of wastewater sludge: change in drying area owing to volume shrinkage and crack development. *Drying Technology* **2005**, 23(3), 669–682.
9. Tao, T.; Peng, X.F.; Lee, D.J. Structure of crack in thermally dried sludge cake. *Drying Technology* **2005**, 23(7), 1555–1568.
10. Tao, T.; Peng, X.F.; Lee, D.J. Skin layer on thermally dried sludge cake. *Drying Technology* **2006**, 24(8), 1047–1052.
11. Arlabosse, P.; Chavez, S.; Lecomte, D. Method for thermal design of paddle dryers: Application to municipal sewage sludge. *Drying Technology* **2004**, 22(10), 2375–2393.
12. Reyes, A.; Eckholt, M.; Troncoso, F.; Efremov, G. Drying kinetics of sludge from a wastewater treatment plant. *Drying Technology* **2004**, 22(9), 2135–2150.
13. Font, R.; Gomez-Rico, M.F.; Fullana, A. Skin effect in the heat and mass transfer model for sewage sludge drying. *Separation and Purification Technology* **2011**, 77(1), 146–161.
14. Bennamoun, L.; Crine, M.; Léonard, A. Convective drying of wastewater sludge: Introduction of shrinkage effect in mathematical modeling. *Drying Technology* **2013**, 31(6), 643–654.
15. Bennamoun, L.; Fraikin, L.; Léonard, A. Modeling and simulation of heat and mass transfer during convective drying of wastewater sludge with introduction of shrinkage phenomena. *Drying Technology* **2014**, 32(1), 13–22.
16. Hsu, J.P.; Tao, T.; Su, A.; Mujumdar, A.S.; Lee, D.J. Model for sludge cake drying

accounting for developing cracks. *Drying Technology* **2010**, 28(7), 922–926.

17. Léonard, A.; Meneses, E.; Le Trong, E.; Salmon, T.; Marchot, P.; Toye, D.; Crine, M. Influence of back mixing on the convective drying of residual sludges in a fixed bed. *Water Research* **2008**, 42(10–11), 2671–2677.
18. Berghel, J.; Renstrom, R. Basic design criteria and corresponding results performance of a pilot-scale fluidized superheated atmospheric condition steam dryer. *Biomass and Bioenergy* **2002**, 23(2), 103–112.
19. Srinivasakannan, C.; Balasubramaniam, N. Drying of rubber wood sawdust using tray dryer. *Particulate Science and Technology* **2006**, 24(4), 427–439.
20. Arlabosse, P.; Ferrasse, J.H.; Lecomte, D.; Crine, M.; Dumont, Y.; Léonard, A. Efficient sludge thermal processing: from drying to thermal valorization. In Modern Drying Technology, Volume 4: Energy Savings, Tsotsas, E.; Mujumdar, A.S. Eds., Wiley-VCH, Weinheim, Germany, 2011, 295–329.
21. Garboczi, E.J. Three-dimensional mathematical analysis of particle shape using X-ray tomography and spherical harmonics: Application to aggregates used in concrete. *Cement and Concrete Research* **2002**, 32(10), 1621–1638.
22. Denis, E.P.; Barat, C.; Jeulin, D.; Ducottet, C. 3D complex shape characterization by statistical analysis: Application to aluminium alloys. *Materials Characterization* **2008**, 59(3), 338–343.
23. Lin, C.L.; Miller, J.D. 3D characterization and analysis of particle shape using X-ray microtomography (XMT). *Powder Technology* **2005**, 154(1), 61–69.
24. Job, N.; Sabatier, F.; Pirard, J.P.; Crine, M.; Léonard, A. Towards the production of carbon xerogel monoliths by optimizing convective drying conditions. *Carbon* **2006**,

44(12), 2534–2542.

25. Aferka, S.; Marchot, P.; Crine, M.; Toye, D. Interfacial area measurement in a catalytic distillation packing using high energy X-ray CT. *Chemical Engineering Science* **2010**, 65(1), 511–516.
26. Almazán, M.C.; Léonard, A.; López-Garzón, J.; Abdullah, J.; Marchot, P.; Blacher, S. 3D characterisation of the structure of activated carbon packed beds using X-ray microtomography. 3rd International Workshop on Process Tomography (IWPT-3), April 17–19, 2009, Tokyo, Japan.
27. Toye, D.; Marchot, P.; Crine, M.; Pelsser, A.M.; L'Homme, G. Local measurements of void fraction and liquid hold-up in packed columns using X-ray computed tomography. *Chemical Engineering and Processing* **1998**, 37(6), 511–520.
28. ASAE. ASAE Standard no. D245.5. American Society of Agricultural Engineers, Eds.; St. Joseph, MI, USA, 1996, 452–464.
29. Fraikin, L.; Herbreteau, B.; Chaucherie, X.; Nicol, F.; Crine, M.; Léonard, A. Impact of storage at 4 °C on the study of sludge drying emissions. 2nd European Conference on Sludge Management, September 9–10, 2010, Budapest, Hungary.
30. Li, J.; Bennamoun, L.; Fraikin, L.; Salmon, T.; Toye, D.; Schreinemachers, R.; Léonard, A. Analysis of the shrinkage effect on mass transfer during convective drying of sawdust/sludge mixtures. *Drying Technology* **2014**, 32(14), 1706–1717.
31. Léonard, A.; Blandin, G.; Crine, M. Importance of rheological properties when drying sludge in a fixed bed. In 4th Inter-American Drying Conference: challenges for efficient drying processes, Montreal, Canada, 2009, 258–263.
32. Toye, D.; Crine, M.; Marchot, P. Imaging of liquid distribution in reactive distillation

packings with a new high-energy X-ray tomograph. *Measurement Science and Technology* **2005**, 16(11), 2213–2220.

33. Otsu, N. A threshold selection method from gray-level histograms. *IEEE Transactions on Systems, Man, and Cybernetics* **1979**, 9(1), 62–67.
34. Huron, Y.; Salmon, T.; Blandin, G.; Crine, M.; Léonard, A. Effect of liming on the convective drying of urban residual sludges. *Asia-Pacific Journal of Chemical Engineering* **2010**, 5(6), 909–914.
35. Vaxelaire, J.; Puiggali, J.R. Analysis of the drying of residual sludge: From the experiment to the simulation of a belt dryer. *Drying Technology* **2002**, 20(4–5), 989–1008.
36. Sherwood, T.K. The drying of solids – II. *Industrial and Engineering Chemistry* **1929**, 21(10), 976–980.
37. Deng, W.; Li, X.; Yan, J.; Wang, F.; Chi, Y.; Cen, K. Moisture distribution in sludges based on different testing methods. *Journal of Environmental Sciences* **2011**, 23(5), 875–880.
38. Li, J.; Fraikin, L.; Salmon, T.; Plougonven, E.; Toye, D.; Léonard, A. Convective drying behavior of sawdust-sludge mixtures in a fixed bed. In *the fourth European conference on sludge management -ECSM 2014*, May 26–27, 2014, İzmir, Turkey.
39. Schultz, P.; Schlünder, E.U. Influence of additives on crust formation during drying, influence of additives on crust formation during drying. *Chemical Engineering and Processing: Process Intensification* **1990**, 28(2), 133–142.
40. Gac, J.M.; Gradoń, L. A distributed parameter model for the spray drying of multicomponent droplets with a crust formation. *Advanced Powder Technology* **2013**,

24(1), 324–330.

Table 1: Characteristics of the sludge used.

Product	Sludge origin	Initial moisture content	Volatile solids
Sludge	WWTP of Grosses Battes, Liège, Belgium	5.90 kg/kg of dry matter	63.79% in total solid

Table 2: Size distribution of the sawdust used.

Diameter	<0.6 mm	0.6–1.7 mm	1.7–5 mm
Mass percent (%)	20.14%	45.03%	34.83%

Table 3: Drying characteristics of sludges and sawdust/sludge mixtures.

Drying temperature (°C)	Sample	Total amount of sludge (g)	Normalized amount of sludge	*Sludge flow rate	Total amount of evaporated water (g)	Normalized amount of water	**Drying time 95% DS (s)	Normalized drying time	Average drying rate (g/s)	Normalized drying rate
50	Original sludge	500	1.000	1.000	425	1.000	14910	1.000	0.029	1.000
	Mixed sludge	500	1.000	1.000	426	1.003	19970	1.339	0.021	0.749
	Mass ratio =1/9	489	0.978	1.022	420	0.989	17470	1.172	0.024	0.844
	Mass ratio =2/8	475	0.950	1.053	414	0.973	12950	0.869	0.032	1.121

	Mass ratio =3/7	459	0.918	1.089	404	0.950	11450	0.768	0.035	1.237
	Mass ratio =4/6	439	0.878	1.139	390	0.917	8430	0.565	0.046	1.622
80	Original sludge	500	1.000	1.000	424	1.000	5370	1.000	0.079	1.000
	Mixed sludge	500	1.000	1.000	426	1.005	7130	1.328	0.060	0.759
	Mass ratio =1/9	489	0.978	1.022	422	0.995	5970	1.112	0.071	0.899
	Mass ratio =2/8	475	0.950	1.053	411	0.969	4770	0.888	0.086	1.089
	Mass ratio =3/7	459	0.918	1.089	407	0.960	4280	0.797	0.095	1.203

	Mass ratio =4/6	439	0.878	1.139	395	0.932	3720	0.693	0.106	1.342
110	Original sludge	500	1.000	1.000	429	1.000	4510	1.000	0.095	1.000
	Mixed sludge	500	1.000	1.000	429	0.999	5870	1.302	0.073	0.768
	Mass ratio =1/9	489	0.978	1.022	423	0.985	4880	1.082	0.087	0.911
	Mass ratio =2/8	475	0.950	1.053	416	0.970	4010	0.889	0.104	1.091
	Mass ratio =3/7	459	0.918	1.089	400	0.932	3070	0.681	0.130	1.369
	Mass ratio =4/6	439	0.878	1.139	392	0.913	2650	0.588	0.148	1.553

* Sludge flow rate: The inverse value of the normalized amount of sludge. For the mixtures, if the same amount of sludge is treated, the sludge flow rate should be increased.

**Drying time $95\%_{DS}$: The drying time that the dry solid content (DS) reaches 95%.

Table 4: Linear fitting results of the bed volume.

Condition	Drying temperature (°C)	R^2	Equation
Wet	50	0.9396	y = 0.458x + 0.919
	80	0.8982	y = 0.400x + 0.916
	110	0.8973	y = 0.404x + 0.964
Dry	50	0.9835	y = 0.590x + 0.416
	80	0.9849	y = 0.575x + 0.438
	110	0.9910	y = 0.602x + 0.472

Table 5: Linear fitting results of the bed volume shrinkage.

Drying temperature (°C)	R^2	Equation
50	0.9689	y = -31.129x + 54.030
80	0.9891	y = -32.942x + 51.648
110	0.9561	y = -32.998x + 50.410

Table 6: Linear fitting results of the void fraction.

Condition	Drying temperature (°C)	R^2	Equation
Wet	50	0.9313	y = 18.858x + 36.446
	80	0.8897	y = 24.419x + 33.212
	110	0.9292	y = 27.399x + 34.490
Dry	50	0.8570	y = -13.218x + 68.474
	80	0.9942	y = -6.8451x + 62.819
	110	0.6180	y = -4.2638x + 60.614

Table 7: Final void volumes ($\times 10^{-4}$ m^3) of sludges and sawdust/sludge mixtures.

Sample	50 °C	80 °C	110 °C
Original sludge	2.87	2.89	3.51
Mixed sludge	3.03	2.95	3.31
Mass ratio=1/9	3.72	3.36	3.62
Mass ratio=2/8	3.90	4.05	3.87
Mass ratio=3/7	4.14	4.50	4.87
Mass ratio=4/6	5.40	5.10	5.21

Table 8: Linear fitting results of the total exchange surface.

Condition	Drying temperature (°C)	R^2	Equation
Wet	50	0.9738	y = 0.232x + 0.158
	80	0.9351	y = 0.203x + 0.159
	110	0.9927	y = 0.252x + 0.165
Dry	50	0.9900	y = 0.184x + 0.110
	80	0.9856	y = 0.125x + 0.146
	110	0.9472	y = 0.161x + 0.152

Figure 1: Convective pilot-scale dryer.

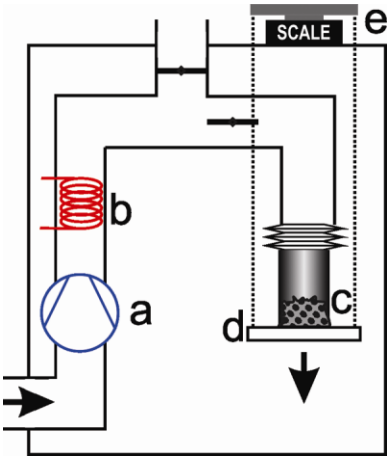

Figure 2: Drying rate vs. moisture content of sludge.

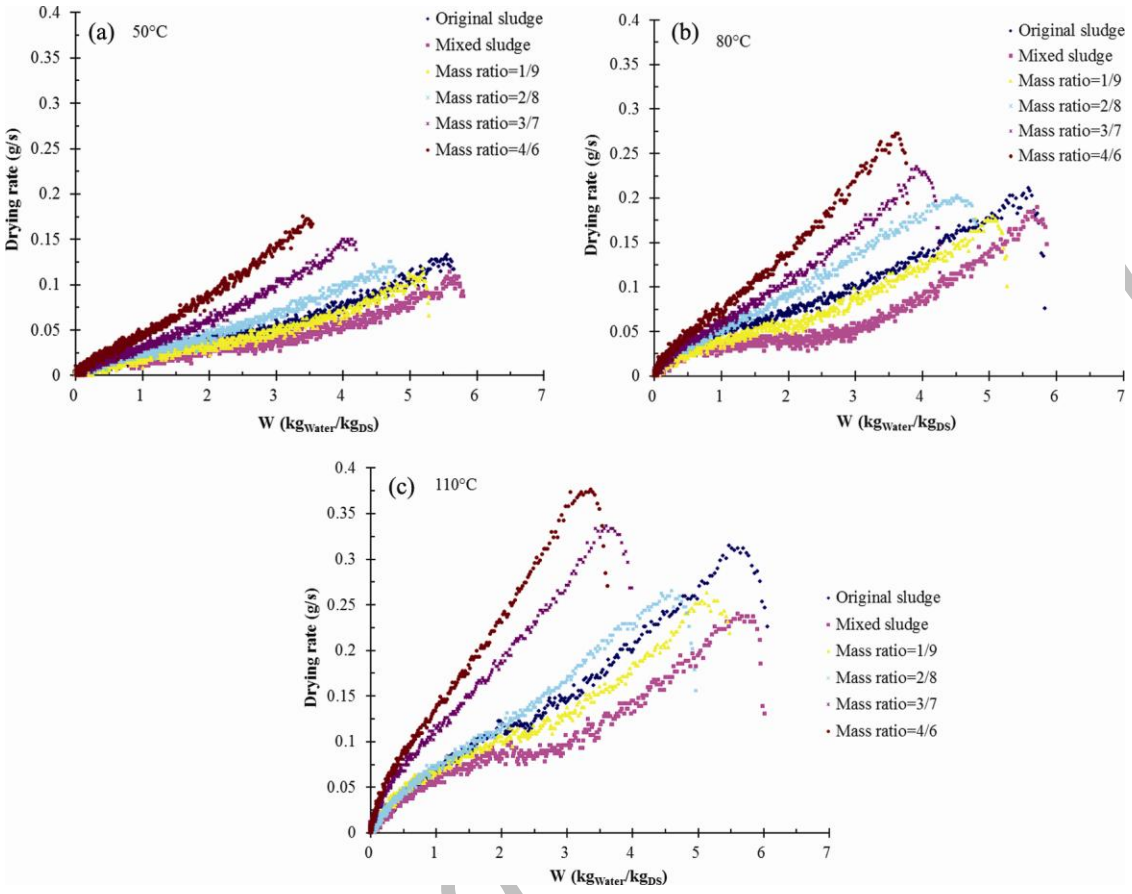

Figure 3: The 2D cross-section (a) and 3D reconstruction image (b) of the bed of the original sludge before drying.

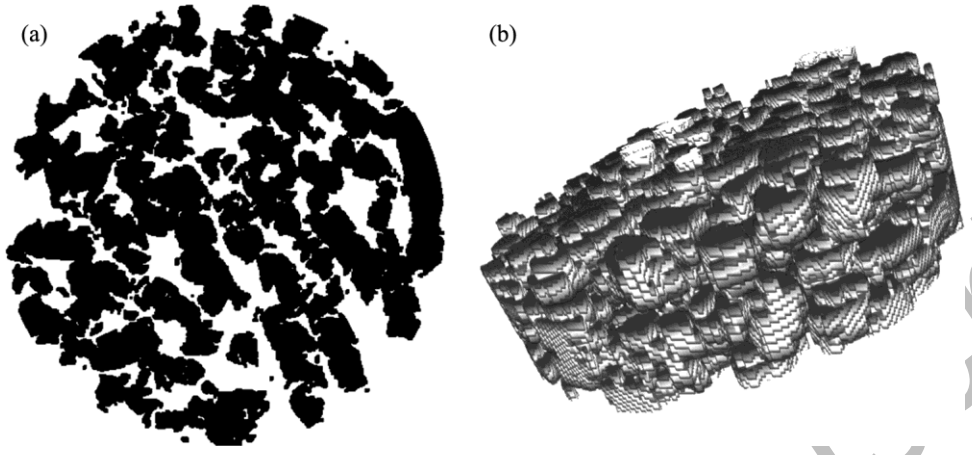

Figure 4: Bed volume before and after drying vs. ratio of sawdust/sludge. □ 50 °C, wet; ◇ 50 °C, dry; △ 80 °C, wet; ▫ 80 °C, dry; ▭ 110 °C, wet; ○ 110 °C, dry. The solid symbols are the original sludge and the hollow symbols are the mixed sludge and sawdust/sludge mixtures.

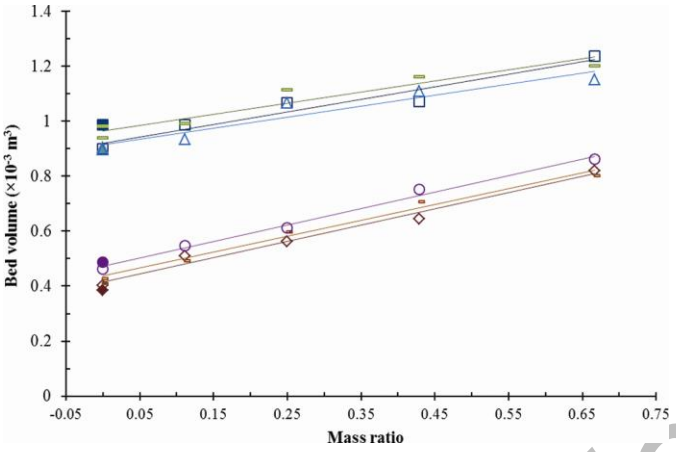

Figure 5: Bed volume shrinkage after drying vs. ratio of sawdust/sludge. □ 50 °C; △ 80 °C; ═ 110 °C. The solid symbols are the original sludge and the hollow symbols are the mixed sludge and sawdust/sludge mixtures.

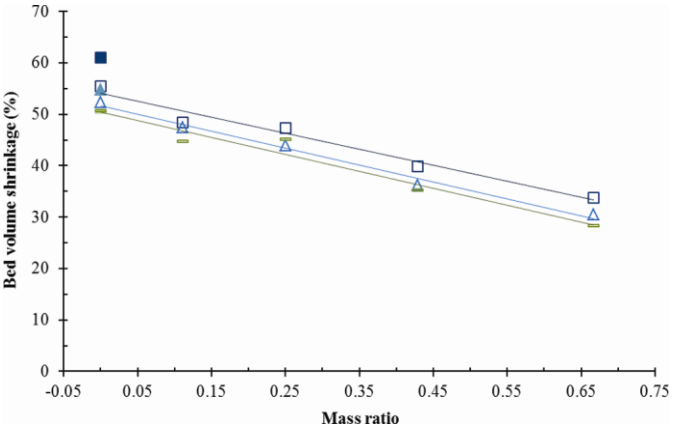

Figure 6: Void fraction before and after drying vs. ratio of sawdust/sludge. □ 50 °C, wet; ◇ 50 °C, dry; △ 80 °C, wet; ▫ 80 °C, dry; ▭ 110 °C, wet; ○ 110 °C, dry. The solid symbols are the original sludge and the hollow symbols are the mixed sludge and sawdust/sludge mixtures.

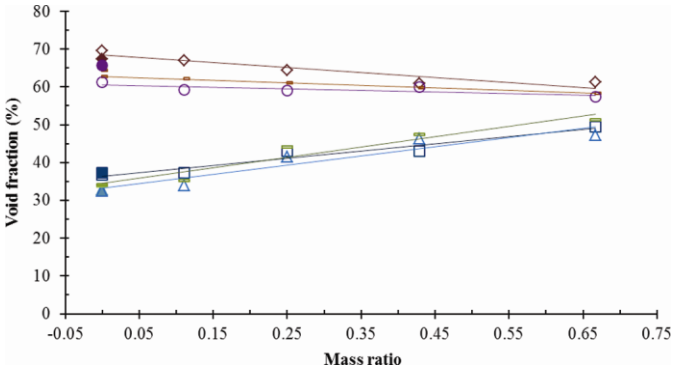

Figure 7: Total exchange surface before and after drying vs. ratio of sawdust/sludge. □ 50 °C, wet; ◇ 50 °C, dry; △ 80 °C, wet; ▫ 80 °C, dry; ▭ 110 °C, wet; ○ 110 °C, dry. The solid symbols are the original sludge and the hollow symbols are the mixed sludge and sawdust/sludge mixtures.